The Journal of Engine Research, Vol. 41 (Winter 2016), pp. 31-39

The Journal of Engine Research

Journal Homepage: www.engineresearch.ir

Research on modification of cooling passage for a 4-cylinder turbo-charged SI engine with precise cooling view point

R. Hemmatkhanloo[1], A. Mohammadi[2*], Mostafa Varmazyar[3]

[1]*KNT University of Technology, Tehran, Iran, reza_hemmatkhanlou@mailfa.com*
[2]*Shahid Rajaee Teacher Training University, Tehran, Iran, a_mohammadi@ip-co.com*
[3]*Shahid Rajaee Teacher Training University, Tehran, Iran, varmazyar.mostafa@srttu.edu*
[*]*Corresponding Author*

ARTICLE INFO

Article history:
Received: 20 December 2015
Accepted: 17 February 2016

Keywords:
Heat transfer
Cooling passage
Turbo-charged engine
Head gasket

ABSTRACT

With the development of engine technology, modern engine power has been improved a lot. Therefore more precise analysis is of much importance. There is more emphasis put on the research on the design of cooling system. An efficient way to study heat transfer in cooling passage of an engine is CFD calculation. With CFD analysis flow pattern in coolant jacket could be analyzed. In this research the velocity, pressure and heat transfer coefficient distribution in the cooling passage of a 4-cylinder SI engine are computed via CFD code AVL Fire. The main goal of author's work is to investigate the precise cooling. Therefore, the effects of head gasket holes on the flow distribution in the hot spot critical regions of the cylinder head can be seen. Three different schemes are proposed to enhance the flow distribution in cylinder head and finally the results are discussed.

1) Introduction

Modern perfect cooling system should be in the best heat state even in different temperature and operation, which is too cold or too hot and can integrate good drive and economy with good reliability [1,2]. This work is made in two steps. Firstly AVL Fire simulation software has been used in the 3D CFD analysis, and velocity, pressure and heat transfer coefficient distributions of the coolant jacket have been obtained and assessed [3]. Then modifications of the head gasket are tested to assess the velocity improvement in critical regions. Mulemane and Soman [4] simulated the cooling circuit of diesel engine based on 1D-3D coupling and predicted realistic flow rates through the cooling jacket and boundary condition for thermal analysis, are obtained from in-cylinder simulations and effect of nucleate boiling on heat transfer was discussed. You-chang, Xiao-hong and Dan [5] used CFD calculation to study cooling system of diesel engine, 3D for coolant jacket and 1D cooling system simulation. The results showed velocity, pressure and heat transfer coefficients distribution in the coolant jacket and could optimize cooling system performance. Lee [6] used experimental flow-loop data and suggested a correction factor on forced convection component of Chen correlation. Li, Fu, Liu, Liu, Cheng [7] used the concept of void fraction and homogeneous flow model for boiling heat transfer with hexahedral element of the flow field. The model based on the assumption that the boiling liquid field is a single phase flow, in which vapor and liquid are homogeneously mixed with void fraction being calculation basis to reflect boiling heat transfer. Their result showed that heat transfer coefficient considering boiling factor is evidently different from that of pure heat convection, and the maximum deviation can be more than fifty percent. Ajotikar, Eggart, Miers [8] investigated nucleate boiling in the cooling passages of an IC engine cylinder head in a computational and experimental domain.

2) Three dimensional CFD analysis for cooling passage

The target engine is a 4-stroke turbocharged SI engine, its Bore/Stroke is 78.6mm/84mm, and rated power/rated speed is 110kW/5500rpm. The cooling passage geometry is made up of cylinder block, head gasket and cylinder head. 3D model of cooling passage is shown in Figure 1. Grid has been generated Gambit software. Mesh model is shown in Figure 2. Approximately 302,000 cells are generated which are mainly Tet cells.

3) Governing Equations

The 3D fluid dynamics calculations were carried out via CFD code AVL Fire. The flow of the coolant is regarded as incompressible, viscid and turbulent. To take the effects of the turbulence into account, AVL Fire offers two different turbulence models, the $k-\varepsilon$ model has been chosen for its robustness and simplicity.

Three governing equations are as follows:

Equation of the quantity

$$\nabla.\vec{V} = 0 \quad (1)$$

Equation of the motion

$$\rho\frac{D\vec{V}}{Dt} = \rho\vec{F} - \nabla P + \mu\Delta\vec{V} \quad (2)$$

Equation of the energy

$$\rho c_p\frac{D\vec{T}}{Dt} = \emptyset + k\Delta T + \rho q \quad (3)$$

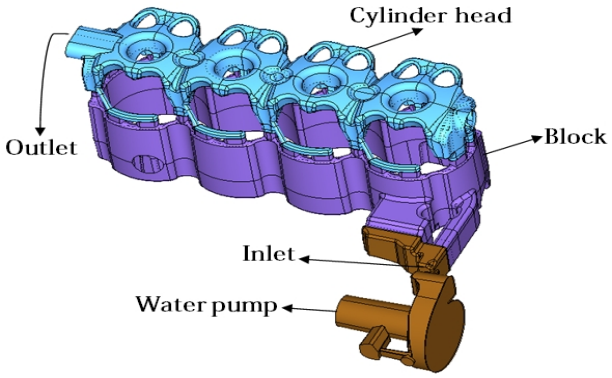

Figure 1: 3D model of cooling passage

Figure 2: Front view of volume grid of cooling jacket

4) Mathematical formulation of sub cooled boiling flow

Many models suggested for sub-cooled flow boiling assume the total wall heat flux q_{w} to be superimposed of two additive contributions, which can be written as

$$q_w = q_{fc} + q_{nb} \quad (4)$$

The first term q_{fc} is due to forced convection, the latter q_{nb} is due to nucleate boiling.

Among the superposition models, the model (Eq. 2) proposed by Chen [8] is widely used today especially in engineering applications in the automotive industry.

$$q_w = q_{fc}\varphi + q_{nb}S \quad (5)$$

Where the two correction parameters φ and S modify the forced convection heat flux q_{fc} and nucleate

boiling heat flux q_{nb}, respectively. Both heat fluxes are computed following Chen's proposal. Accordingly, the first is written as

$$q_{fc} = h_{fc}(T_w - T_b) \quad (6)$$

Where the heat transfer coefficient h_{fc} is calculated using the Dittus-Boelter equation

$$Nu_{fc} = \frac{h_{fc}d_{hyd}}{\lambda_l} = 0.023Re_l^{0.8}Pr_l^{0.4} \quad (7)$$

Involving the bulk flow Reynolds number and the Prandtl number of the liquid phase, respectively.

$$Re_l = \frac{\rho_l u_b d_{hyd}}{\mu_l}, \qquad Pr_l = \frac{\mu_l c_{p,l}}{\lambda_l} \quad (8)$$

The factor φ occurring in Eq. (4) represents the enhancement of the convective component due to bubble agitation. Chen [8] derived a graphic relationship for φ as a dependent of the inverse of the Martinelli number X_{tt}, which reads

$$\left(\frac{1}{X_{tt}}\right) = \left(\frac{\xi_g}{1-\xi_g}\right)^{0.9}\left(\frac{\rho_l}{\rho_g}\right)^{0.5}\left(\frac{\mu_g}{\mu_l}\right)^{0.1} \quad (9)$$

Where ξ_{g} denotes mass fraction of the vapor. Butterworth [5] fitted this relationship $\varphi = \varphi\left(\frac{1}{X_{\mathrm{tt}}}\right)$ with

$$\xi_g > 0: \quad \varphi = 2.35\left(\frac{1}{X_{tt}} + 0.213\right)^{0.736} \quad (10)$$

$$\xi_g \le 0.1: \quad \varphi = 1$$

In sub-cooled boiling flow the vapor mass fractions are typically small, such that $\xi_{\mathrm{g}} \le 0.1$ applies and φ can be assumed unity. The nucleate boiling heat flux

$$q_{nb} = h_{fc}(T_w - T_s) \quad (11)$$

is obtained using a correlation due to Forster and Zuber [6]

$$h_{nb} = 0.00122\frac{\lambda_l^{0.79}c_{p,l}^{0.45}\rho_l^{0.49}}{\sigma^{0.5}\mu_l^{0.29}h_{lg}^{0.24}\rho_g^{0.24}}\Delta T_{sat}^{0.25}\Delta p_{sat}^{0.75} \quad (12)$$

Where the saturation pressure difference corresponding to the superheat temperature is written as

$$\Delta p_{sat} = p_{sat}(T_w) - p_{sat}(T_{sat}) \quad (13)$$

The essential difference between Chen's approach and the BDL is in the modeling of the modification of the nucleate boiling component in terms of the factor S in Eq. (3). Chen introduced this parameter S as a flow-induced suppression factor, which he correlated as an empirical function of the product $Re_l\varphi^{1.25}$. This correlation was later fitted by Butterworth [5] with the expression

$$S_{Chen} = \frac{1}{1 + 2.53\times10^{-6}(Re_l\varphi^{1.25})^{1.17}} \quad (14)$$

For sub-cooled boiling flow, where $\varphi \approx 1$, the factor S_{Chen} obviously depends on the bulk flow Reynolds number only. In some texts, S_{Chen} is stated as following (figure 3)

$$S_{Chen} = 1 \qquad Re < 1.10^4$$
$$S_{Chen} = 3.4 - 0.6\,log(Re) \qquad 1.10^4 \le Re \le 4.10^5$$
$$S_{Chen} = 3.876\times10^{-2} \qquad Re > 4.10^5$$

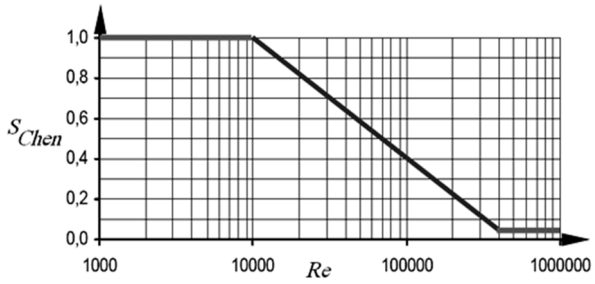

Figure 3: Chen suppression factor

The Chen model provides a good description of the wall heat transfer enhancement due to nucleate boiling. Meanwhile it does not provide a correct description of the heat flux saturation that occurs when ΔT_{sat} increases and the fluid enters in the transition boiling region. In that case, the Chen correlation predicts a continuously increasing heat flux instead of the physical saturation. The main deficiency of Chen model is located on the suppression factor. As a function of a Reynolds number of the global geometry, it cannot take the local fluid state into account. In particular, the effect of heat flux saturation while approaching the boiling transition region cannot be predicted.

The Boiling Departure Lift-off model is a recent improvement [7] in which the suppression factor is computed from local velocity and length scales.

In the BDL model the suppression factor is decomposed in two parts

$$S_{BDL} = S_{BDL1}S_{BDL2} \quad (15)$$

First suppression factor

The modeling of the first suppression factor S_{BDL1} is based on the study of bubble growth and dynamics [8]. Fig. (4) describes the process This study assumes that the wall is horizontal. When a bubble is generated on the wall, it starts to grow on a fixed wall point called the *nucleation site*. The set of forces applied on the bubble gives it a droplet shape with the axis slightly inclined downstream. The angle of the axis with the vertical is θ.

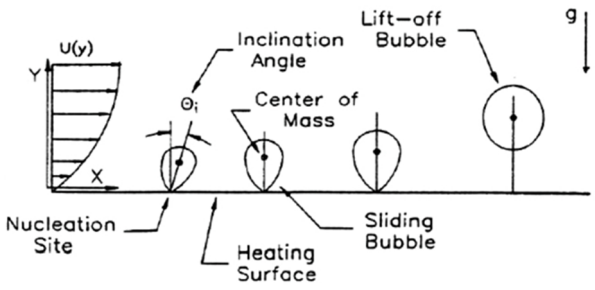

Figure 4: Bubble departure and lift-off

Once the bubble diameter is big enough, the bubble starts to slide downstream along the wall though is still attached to the wall. This diameter is called the *Departure Diameter* d_D.
While sliding, the bubble axis comes back to the vertical and the bubble still grows until its diameter is big enough to allow the bubble to leave the wall. This is the Lift-off and the corresponding diameter is called the *Lift-off Diameter* d_L.
The first suppression factor is then defined as:

$$S_{BDL1} = (\frac{d_D}{d_L})^n \quad (16)$$

Where the exponent n has been calculated from model calibration.

Departure and lift-off diameters

Figure 5 shows the forces influencing the bubble growth (some other forces exist but they are negligible).

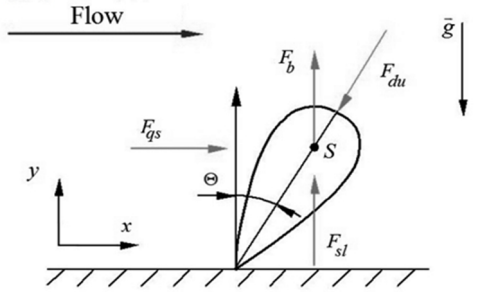

Figure 5: Forces applied on a bubble

These forces are:
The growth force F_{du} :

$$F_{du} = -\rho_l(T_{sat})4b^4Ja^4(\frac{\lambda}{\rho_l C_p})^2\frac{1}{\pi}(\frac{3}{2}C_s - 1) \quad (17)$$

Where the Jakob number is defined as:

$$Ja = \frac{\rho(T_{sat})c_p(T_{sat})(T_w - T_{sat})}{\rho_v(T_{sat})L_v(T_{sat})} \quad (18)$$

The buoyancy forceF_{bcy}:

$$F_{bcy} = \frac{4}{3}\pi r^3\big(\rho_l(T_{sat}) - \rho_v(T_{sat})\big)g \quad (19)$$

The buoyancy force F_{bcy}:

$$F_{bcy} = \frac{4}{3}\pi r^3\big(\rho_l(T_{sat}) - \rho_v(T_{sat})\big)g \quad (20)$$

Where g is the gravity acceleration and r the bubble radius.
The quasi-steady drag force F_{qs}:

$$F_{qs} = 6\pi\rho_l(T_{sat})\frac{\mu_l}{\rho_l}u_r r[\frac{2}{3} + \Big[(\frac{12}{Re_{bub}})^m + 0.796^m\Big]^{-\frac{1}{m}}] \quad (21)$$

Where u_r is the velocity at the bubble center and Re_b is the bubble Reynolds number. The bubble velocity is estimated. The shear lift force F_{sl}:

$$F_{sl} = \frac{1}{2}\rho_l u_r^2\pi r^2 3.877\sqrt{G_s}(\frac{1}{Re_{bub}^2} + 0.014G_s^2)^{0.25} \quad (22)$$

Where G_s is the shear rate. When the bubble starts to slide on the wall, it is assumed that its velocity is the same as the liquid around. Therefore the bubble velocity u_r and the velocity gradient in the shear rate G_s are estimated due to the Reichart law of the wall.

Second suppression factor

The second suppression factor is a correction to the definition of the pool boiling coefficient h_{pool}. In the Eq. (5) the temperature and pressure differences refer to the wall temperature while the bubble center is not exactly on the wall. As shown in Fig. (6) the correct relation should be:

$$h_{pool} = 0.00122[\frac{C_p^{0.45}\lambda^{0.79}\rho_l^{0.49}}{L_v^{0.24}\rho_v^{0.24}\sigma^{0.5}\mu^{0.29}}]\Delta T_{eff}^{0.24}\Delta P_{eff}^{0.75} \quad (23)$$

With ΔT_{eff} and ΔP_{eff} referring to the bubble center temperature.
These considerations give rise to the derivation of S_{BDL2}:

$$S_{BDL2} = \frac{S_{BDL1}h_{pool}}{1 + C_{BDL}Nu} \quad (24)$$

Where Nu is a bubble Nusselt number.

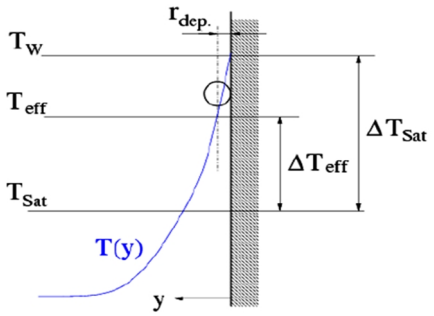

Figure 6: Definition of effective temperature and pressure

5) Boundary conditions

The inlet of the coolant is defined as a constant velocity with 2 m/s at temperature of 85 [C]. The outlet of the coolant is zero gradient. The coolant is a mixture of water/ethylene glycol (50/50). Wall surface temperature of boundary conditions at the cooling passage surface is imported from the thermal analysis in Abaqus FEM software.

6) CFD calculation results

After CFD calculation analysis, pressure field, coolant velocity and heat transfer coefficient (HTC) distribution for cooling passage can be obtained. Total pressure distribution of coolant in cooling passage is shown in Figure 7.
Total pressure loss of the coolant in cooling passage is mostly due to the head gasket coolant holes. From calculation results the total pressure drop between inlet and outlet of the cooling jacket is about 31 kPa which is measured 35 kPa in practice. Seen in a whole, pressure field of cooling passage in cylinder head is almost uniform in four cylinders.

Velocity field contours in cooling passage are shown in Figures 8 to 10. The maximum velocity is 4.39 $^{m}/_{s}$ which occurs in the head gasket coolant holes linking the block to cylinder head. Because of the high exhaust gas temperature and the narrow bridge between the two exhaust valve seats, especially the area around the exhaust is one of the critical zones.
As shown in Figure 8, the coolant is pumped from the bottom of the first cylinder, and thus causes the water flow velocity in the fourth cylinder slower obviously, and the velocity of the coolant flow from the bottom of the first cylinder to the fourth cylinder is gradually slower, so does the velocity of coolant flow from the upper of the first cylinder to the fourth, which makes the cooling equilibrium in each cylinder. Energy calculation results show that HTC distribution trend of coolant flow for engine cooling passage accords with velocity field distributions. Distribution of the HTC of coolant are shown in Figures 11.

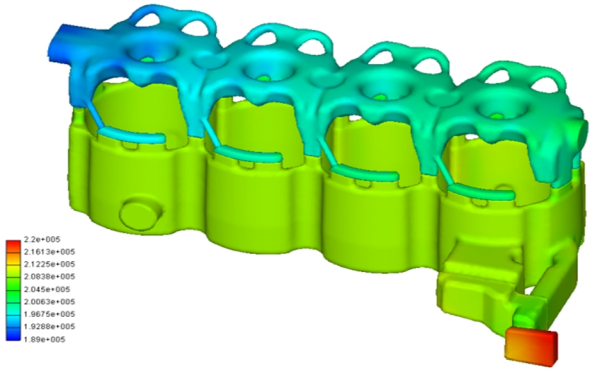

Figure 7: Total pressure distribution in the cooling passage

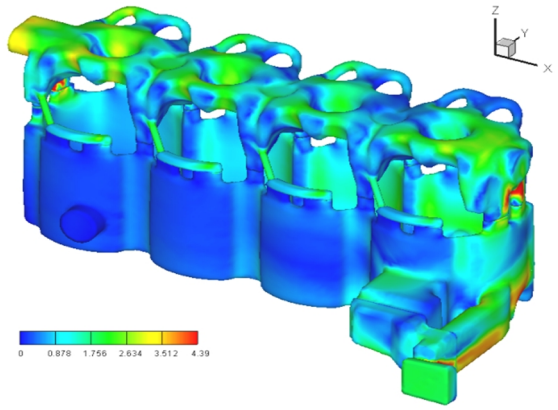

Figure 8: 3D view of velocity in cooling passage

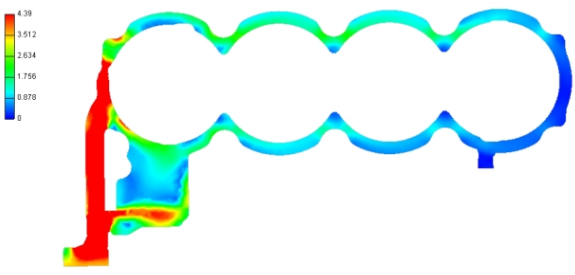

Figure 9: Section view of velocity in cooling passage

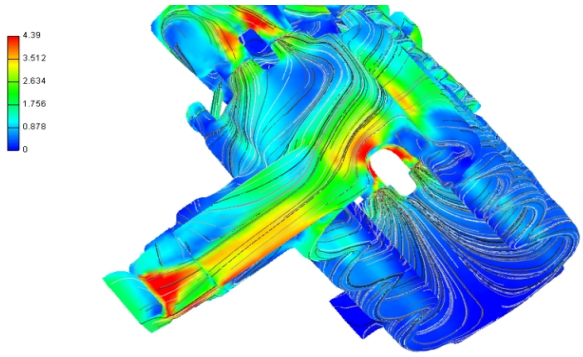

Figure 10: Path-lines showing flow development through the cooling passage

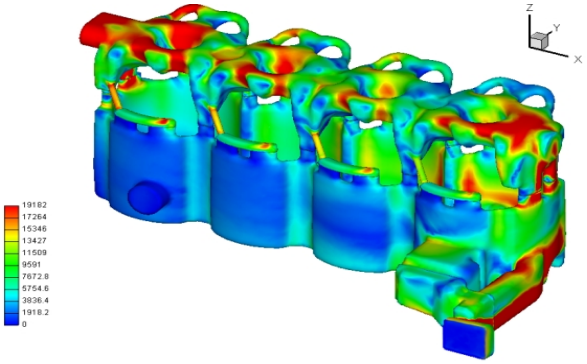

Figure 11: HTC distribution of coolant in cooling passage

7) Improved Design Comparison of Head Gasket Holes Configurations

The main objective of this paper is to investigate the effects of blocking the head gasket holes on the coolant velocity distribution in critical regions of cylinder head. These critical regions are depicted on Figure 12 by letters A, B, C & D. It is obvious that the regions in the exhaust side are of much importance. As we know, low flow velocity in valve bridge will make the heat transfer coefficient fall down, great quantities of heat is difficult to send out, so the cooling passage structure must be modified.

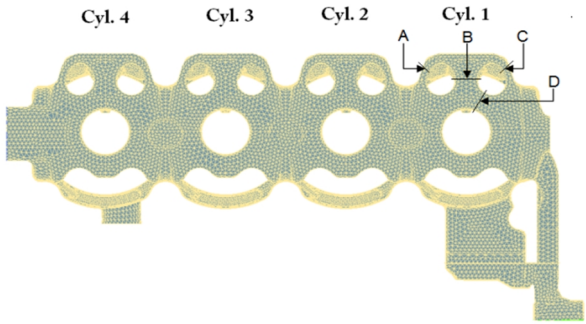

Figure 12: Critical zones of head cylinder cooling passage

Two strategies can be considered: 1) using precision cooling, 2) manipulating the cooling system partially. Cooling passages in conventional engines are typically formed by the space left over once other features have been designed. This results in relatively large volumes of coolant concentrated in locations of both high and low heat flux. The potential benefits of maintaining a lower distribution of metal

temperatures are an increase to engine power fuel economy, better volumetric efficiency as well as reduced wear of engine components due to a reduction of thermal distortion. Control of metal temperature can be improved by careful design of cooling passage. Local coolant velocities can be determined from knowledge of heat flux profiles then the required local velocities can be obtained by choosing the correct flow pattern and local cross sectional areas in the cooling passage.

Although precision cooling is an established research technique offering all the benefits mentioned above. To the date, there is currently no application in production employing precision cooling in SI engines due to additional cost and difficulties in manufacturing process. The second strategy is modifying the cooling system. As it is unpractical to change the cylinder head structure for the batch-produced engine, head gasket is a very effective engine component that can be used for optimizing coolant flow distribution in both the cylinder block and cylinder head through blocking the head gasket holes at the intake side. A head gasket is a gasket that sits between the engine block and cylinder head to ensure maximum compression and avoid leakage of coolant or engine oil into the cylinders. A great improvement of flow velocity distribution in cylinder body and cylinder head affect the metal temperature greatly. Geometry of the EF7 TC head gasket is shown in Figure 14. Coolant holes are numbered 1-16. In the cooling passage, percentages of inlet flow rate passing through each gasket hole are measured (table 1).

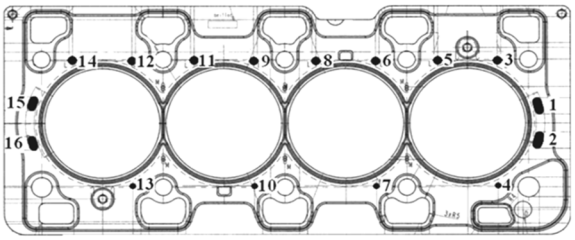

Figure 14: EF7-TC head gasket

Figure 15 derived from [8] shows the relationship between coolant velocity and metal temperature for constant heat fluxes. Higher flow velocity will make the metal temperature fall down.

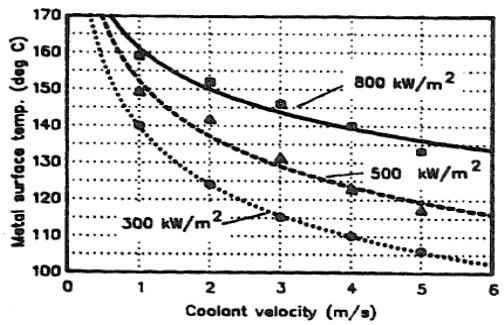

Figure 15: Effects of coolant velocity on metal temperature for various heat fluxes [8]

As mentioned before, a short-cut scheme to improve the flow velocity distribution in head is to block the head gasket holes at the intake side. Here there are three configurations of gasket holes that aim to enhance the flow velocity distribution at critical regions. It should be noted that the coolant gasket holes which links the cylinder block conduits to head ones are depicted in Figure 16 by solid circles and the blocked holes by blank circles.

Table 1: Percentage of inlet flow rate passing through each gasket hole

Hole No.	% inlet flow rate	Hole No.	% inlet flow rate
1	15	9	4
2	15	10	2
3	4	11	4
4	2	12	4
5	4	13	2
6	4	14	4
7	2	15	15
8	4	16	15

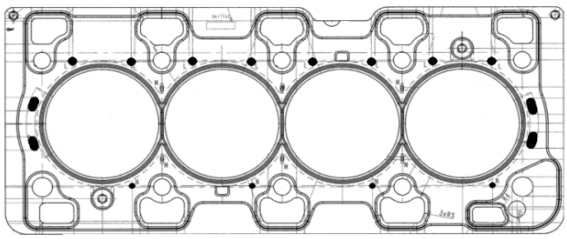

a) EF7 TC original head gasket

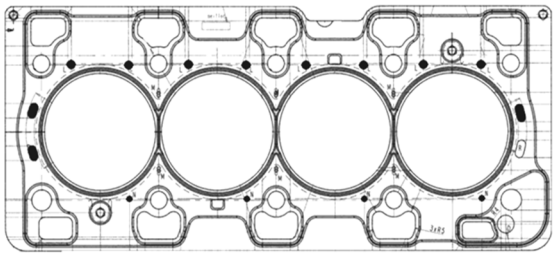

b) 1st scheme

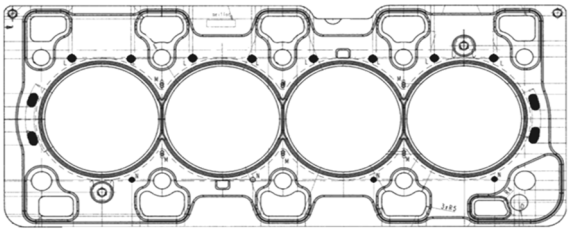

c) 2nd scheme

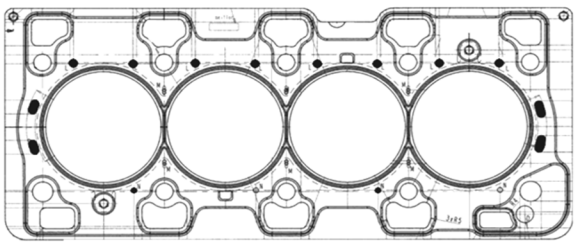

d) 3rd scheme

Figure 16: Various schemes of EF7 TC head gasket and original one

CFD calculation based on the previous mentioned boundary conditions were conducted via AVL Fire software. Flow velocities contours of all cases are shown in Figure 17. Quantitative representation of flow velocity is also illustrated in table 2 for critical points of cylinders 1 to 4. It can be seen, the flow velocity of coolant in almost all desired zones are improved in third scheme.

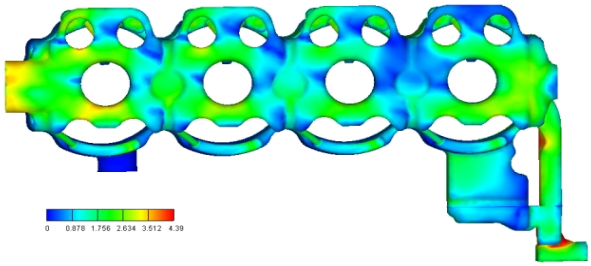

a) Top view of volume grid of cooling jacket

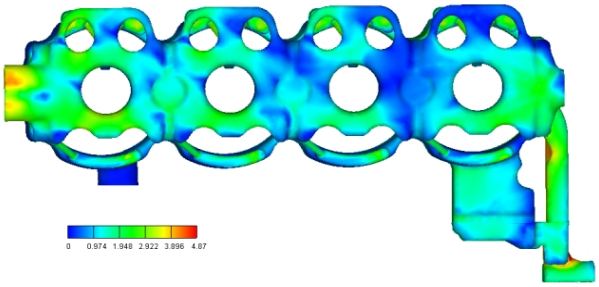

b) Top view of volume grid of cooling jacket

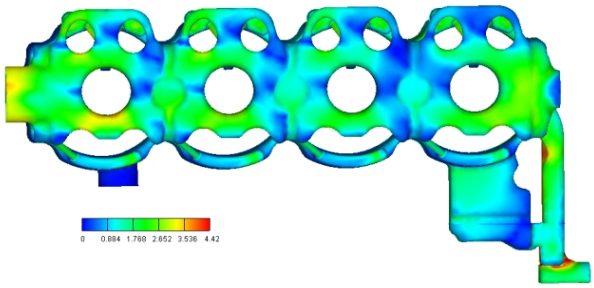

c) Top view of volume grid of cooling jacket

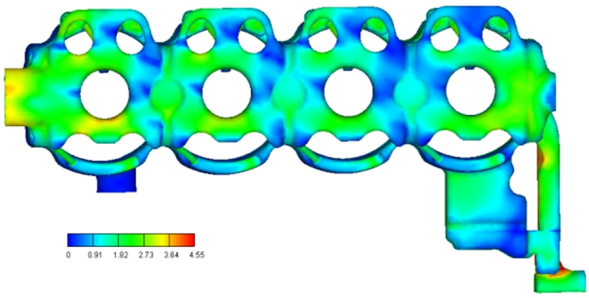

d) Top view of volume grid of cooling jacket

Figure 17: Coolant velocity contours for schemes 1, 2, 3 and original

It is also seen that blocking hole No. 2 in the first scheme carrying 15% of inlet flow rate hazardous. Low flow velocity will make the heat transfer coefficient fall down, great quantities of heat is difficult to be sent out. And the second scheme has not sensitive effect on flow distribution.

The flow velocities of varied cylinder for third scheme is the best distribution among three schemes from CFD calculation. It is also concluded that blocking hole No. 2 in first scheme carrying 15% of inlet flow rate is hazardous. And the second scheme has no sensitive effect on flow distribution.

Table 2: Flow velocity in critical points for different schemes

Zone	Cylinder 1			
	1st scheme	2nd scheme	3rd scheme	Original
A	0.65	0.76	1.58	0.67
B	0.51	0.63	0.99	0.60
C	0.32	0.52	0.78	0.35
D	1.07	1.23	1.53	1.38
Zone	Cylinder 2			
	1st scheme	2nd scheme	3rd scheme	Original
A	1.24	1.29	1.56	1.37
B	0.59	0.45	0.56	0.69
C	0.67	0.82	0.70	0.81
D	0.79	1.29	1.21	1.40
Zone	Cylinder 3			
	1st scheme	2nd scheme	3rd scheme	Original
A	1.32	1.68	1.49	1.60
B	0.59	0.53	0.51	0.54
C	0.79	0.94	0.85	0.98
D	1.45	1.72	1.73	1.70
Zone	Cylinder 4			
	1st scheme	2nd scheme	3rd scheme	Original
A	1.93	2.11	2.10	2.18
B	0.52	0.51	0.54	0.50
C	1.09	1.16	1.18	1.18
D	1.87	2.00	1.85	2.12

Acknowledgment

The authors wish to express their gratitude to the staff of CAE department at Irankhodro Powertrain Company (IPCo.) for their support and assistance.

Nomenclature

c_p	Specific heat capacity of fluid
F	Mass force
k	Thermal conductivity
P	Pressure
q	Heat of spreading to fluid by heat radiation
T	Temperature of the fluid
V	Velocity
μ	Dynamic heat capacity of fluid
$\emptyset$	Energy dissipation function

References

[1]P. Tamamidis and K. Sethupathi. Role of CFD in Heavy Machinery Development, SAE Paper 972718, 1997

[2]F. J. LaimbÖck, Gerhard Meister and Simon Grilc. CFD Application in Compact Engine Development, SAE 982016, 1998

[3] J. Ye, J. Covey, D. D. Agnew. Coolant Flow Optimization in a Racing Cylinder Block and Head Using CFD Analysis and testing. SAE Paper 2004-01-3542, 2004

[4] A. Mulemane, R. Soman, CFD Based Complete Engine Cooling Jacket Development and Analysis, SAE 2007-01-4129, 2007

[5] L. You-chang, G. Xiao-hong, C., Dan, Research on cooling system for 4-cylinder diesel engine, SAE 2007-01-2064, 2007

[6] H. S. Lee, Heat Transfer Predictions using the Chen Correlation on Sub cooled Flow Boiling in a Standard IC Engine", SAE 2009-01-1530, 2009

[7] G. X. Li, Y. Liu, S. Bai, A homogeneous flow model for boiling heat transfer calculation based on single phase flow, Energy Conversion and Management, Vol. 50, Issue. 7, pp. 1862-1868, 2009

[8] N. Ajotikar, B. J. Eggart, S. A. Miers, Nucleate Boiling Identification and Utilization for Improved Internal Combustion Engine Efficiency, ASME 2010. Internal Combustion Engine Division Fall Technical Conference (ICEF2010), pp. 949-958., September 12–15, San Antonio, Texas, USA, 2010

[9] M. J. Clough, Precision Cooling of a Four Valve per Cylinder Engine, SAE paper 931123, 1993

فصلنامهٔ علمی- پژوهشی تحقیقات موتور
تارنمای فصلنامه: www.engineresearch.ir

تحقیق روی اصلاح راهگاه آب در یک موتور چهار استوانه پرخوران با دیدگاه خنک کاری دقیق

رضا همت خانلو[1]، آرش محمدی[2*]، مصطفی ورمزیار[3]

[1] دانشگاه خواجه نصیرالدین طوسی، تهران، ایران reza_hemmatkhanlou@mailfa.com
[2] دانشگاه تربیت دبیر شهید رجایی، تهران، ایران a_mohammadi@ip-co.com
[3] دانشگاه تربیت دبیر شهید رجایی، تهران، ایران varmazyar.mostafa@srttu.edu
[*] نویسندهٔ مسئول

چکیده

با توسعه موتورهای احتراق داخلی، توان موتورها افزایش یافته است و تحلیل دقیق و کاملی از آنها مورد نیاز است. طراحی سامانه خنک کاری تاثیر قابل توجه روی عملکرد موتور دارد. روش مناسب برای مطالعه انتقال حرارت در راهگاه آب یک موتور دینامیک سیالات محاسباتی است. در این تحقیق، توزیع فشار، سرعت و ضریب انتقال حرارت در راهگاه آب یک موتور پرخوران بدست آمده با نرم افزار فایر انجام شده است. هدف اصلی نویسندگان بررسی اثر سوراخهای لایی بستار در توزیع جریان در ناحیه های بحرانی حرارتی بستار می باشد. سه طرح متفاوت برای بهبود توزیع جریان در بستار ارائه شده است. در نهایت روی نتایج بحث شده است

اطلاعات مقاله

تاریخچهٔ مقاله:
دریافت: 30 آذر 1394
پذیرش: 29 بهمن 1394

کلیدواژه‌ها:
انتقال حرارت
راهگاه آب
موتور پرخوران
لایی بستار